$SO(10)$ inspired Z' models at the LHC

Simon J. D. King,* Stephen F. King,† and Stefano Moretti‡
School of Physics and Astronomy, University of Southampton, Southampton SO17 1BJ, United Kingdom

(Received 5 March 2018; revised manuscript received 18 May 2018; published 15 June 2018)

We study and compare various Z' models arising from $SO(10)$, focusing in particular on the Abelian subgroup $U(1)_R \times U(1)_{B-L}$, broken at the TeV scale to Standard Model hypercharge $U(1)_Y$. The gauge group $U(1)_R \times U(1)_{B-L}$, which is equivalent to the $U(1)_Y \times U(1)_\chi$ in a different basis, is well motivated from $SO(10)$ breaking and allows neutrino mass via the linear seesaw mechanism. Assuming supersymmetry, we first consider single step gauge unification to predict the gauge couplings, then we consider the detection and characterization prospects of the resulting Z' at the LHC by studying its possible decay modes into di-leptons as well as into Higgs bosons. The main new result here is to analyse in detail the expected leptonic forward-backward asymmetry at the high luminosity LHC and show that it may be used to discriminate the $U(1)_R \times U(1)_{B-L}$ model from the usual $B-L$ model based on $U(1)_Y \times U(1)_{B-L}$.

DOI: 10.1103/PhysRevD.97.115027

I. INTRODUCTION

$SO(10)$ grand unified theories (GUTs) are very attractive since they predict right-handed neutrinos and make neutrino mass inevitable. Supersymmetry (SUSY) allows for a single step unification of the gauge couplings. Being a rank 5 gauge group, $SO(10)$ also naturally accommodates an additional Z' gauge boson, which may have a mass at the TeV scale within the range of the Large Hadron Collider (LHC). Such Z' models are attractive since, apart from the three right-handed neutrinos, they do not require any new exotic particles to make the theory anomaly free.

There are two main symmetry-breaking patterns of $SO(10)$ leading to the Standard Model (SM) gauge group. First, there is the $SU(5)$ embedding,

$$SO(10) \to SU(5) \times U(1)_\chi \to SU(3)_C \times SU(2)_L \times U(1)_Y \times U(1)_\chi, \quad (1)$$

where the $U(1)_\chi$ is broken at the TeV scale, yielding a massive Z'_χ. For recent examples of models based on such a Z'_χ, see e.g., [1].

Secondly there is the Pati-Salam gauge group embedding,

$$SO(10) \to SU(4)_{PS} \times SU(2)_L \times SU(2)_R. \quad (2)$$

The Pati-Salam color group $SU(4)_{PS}$ may be broken to $SU(3)_C \times U(1)_{B-L}$, leading to the left-right symmetric model gauge group. The $SU(2)_R$ group may be broken to the gauge group $U(1)_R$ associated with the diagonal generator T_{3R}. It is, thus, possible to break $SO(10)$ in a single step at the GUT scale without reducing the rank,

$$SO(10) \to SU(3)_C \times SU(2)_L \times U(1)_R \times U(1)_{B-L}. \quad (3)$$

The resulting gauge group in Eq. (3) does not predict any new charged currents and is not very tightly constrained phenomenologically. It may, therefore, survive down to the TeV scale before being broken to the SM gauge group, leading to the prediction of a massive $Z'_{\rm BLR}$, accessible to the Large Hadron Collider (LHC).

In this paper, we shall focus on $SO(10)$ broken at the GUT scale in a single step, as in Eq. (3). In order to allow for gauge coupling unification, we shall assume supersymmetry (SUSY) which is broken close to the TeV scale, but at a high enough scale to enable the superpartners to have evaded detection at the LHC. We shall be interested in the $Z'_{\rm BLR}$ which emerges when the Abelian subgroup $U(1)_R \times U(1)_{B-L}$ is broken down to the SM hypercharge gauge group $U(1)_Y$ near the TeV scale (for brevity we refer to this scenario as the BLR model). We study the discovery prospects of such a $Z'_{\rm BLR}$ at the LHC, its possible decay mode into Higgs bosons, and the expected forward-backward asymmetry, comparing the predictions to the well studied $B-L$ model based on $U(1)_Y \times U(1)_{B-L}$ [2–6]. We comment on the $U(1)_Y \times U(1)_\chi$ model [7,8] below.

The Abelian gauge group $U(1)_R \times U(1)_{B-L}$ has quite a long history in the literature as reviewed in [8,9]. It was recently realized that SUSY $SO(10)$ models which break down to this gauge group may allow for a new type of

*sjd.king@soton.ac.uk
†king@soton.ac.uk
‡s.moretti@soton.ac.uk

seesaw model, namely the linear seesaw model [10,11]. Subsequently, the phenomenology of the SUSY $U(1)_R \times U(1)_{B-L}$ model has been studied in a number of works [12–18]. Indeed, it has been demonstrated that the Abelian BLR gauge group $U(1)_R \times U(1)_{B-L}$ is equivalent to $U(1)_Y \times U(1)_\chi$ [arising from the breaking chain in Eq. (1)] by a basis transformation and furthermore that this equivalence is preserved under RGE running, when kinetic mixing is consistently taken into account [18]. Therefore, the physics of the TeV scale $Z'_{\rm BLR}$ considered here should be identical to that of the Z'_χ [18].

We emphasize that there are several new aspects of our study including: the statistical significance of producing a $Z'_{\rm BLR}$ at the LHC including finite width and interference effects (the LHC uses a narrow width approximation); the study of Higgs final states in the $U(1)_{B-L} \times U(1)_R$ model; and the study of forward-backward asymmetry at the high luminosity LHC as a discriminator between the $U(1)_R \times U(1)_{B-L}$ model (or equivalently the $U(1)_Y \times U(1)_\chi$ model) and the usual Z'_{BL} based on $U(1)_Y \times U(1)_{B-L}$, i.e., the commonly studied $B-L$ model [2–6].

The layout of the remainder of the paper is as follows. In Sec. II, we discuss the BLR model. In Sec. III, we give the $Z'_{\rm BLR}$ couplings to fermions in this model, while in Sec. IV we give the $Z'_{\rm BLR}$ couplings to Higgs. In Sec. V, we present a renormalization group analysis of the BLR model. In Sec. VI, we present the results for the Drell-Yan production of the Z' in the BLR model, assessing the discovery potential at the LHC, present the leptonic forward-backward asymmetry as a discriminator of different models, and discuss the Higgs final state branching fractions of $Z'_{\rm BLR}$ decays. Section VII concludes the paper.

II. MODEL

We shall not consider the high-energy $SO(10)$ breaking here, so the starting point of the considered model is to assume that, below the GUT scale, we have the gauge group as on the right-hand side of Eq. (3), namely,

$$SU(3)_C \times SU(2)_L \times U(1)_R \times U(1)_{B-L} \tag{4}$$

Note that in this basis the hypercharge gauge group $U(1)_Y$ of the SM is not explicitly present, instead it is "unified" into $U(1)_R \times U(1)_{B-L}$. Note that, although the Abelian factors are equivalent to the $U(1)_Y \times U(1)_\chi$ model by a basis transformation, we shall work in the $U(1)_R \times U(1)_{B-L}$ basis. In order to allow gauge coupling unification, we need SUSY, but we shall assume it is broken above the $Z'_{\rm BLR}$ mass scale so that SUSY particles are not present in the decays of the $Z'_{\rm BLR}$. Note that such SUSY decays have been considered extensively in [12–18].

At the $Z'_{\rm BLR}$ mass scale (typically a few TeV), hypercharge emerges from the breaking,

$$U(1)_R \times U(1)_{B-L} \to U(1)_Y, \tag{5}$$

where the hypercharge generator is identified as

$$Y = T_{3R} + T_{B-L}, \tag{6}$$

where

$$T_{B-L} = (B-L)/2. \tag{7}$$

The symmetry breaking in Eq. (5) requires two Higgs superfields $\chi_{1,2}$ whose scalar components develop vacuum expectation values (VEVs) which carry nonzero T_{3R} and opposite T_{B-L} so that they are neutral under hypercharge. If they arise from an $SU(2)_R$ doublet then this fixes their charges to be $T_{3R} = \pm 1/2$ and hence $T_{B-L} = \mp 1/2$. Two of them with opposite quantum numbers are required by SUSY to cancel anomalies (and for holomorphicity). They must be singlets under both $SU(3)_C$ and $SU(2)_L$ in order to preserve these gauge groups.

Finally, at the electroweak (EW) scale we have the usual Standard Model (SM) breaking

$$SU(2)_L \times U(1)_Y \to U(1)_Q, \tag{8}$$

where the electric charge generator is identified as

$$Q = T_{3L} + Y. \tag{9}$$

As in usual SUSY models, the EW symmetry breaking is accomplished by two Higgs doublets $H_{u,d}$ of $SU(2)_L$ which have $B-L=0$. If the two Higgs doublets of $SU(2)_L$ were embedded into a single $SU(2)_R$ doublet, then we expect that $H_{u,d}$ will have $T_{3R} = \pm 1/2$, respectively. In addition, in order to accomplish neutrino masses via the linear seesaw model, we need to add three complete singlet superfields S, as discussed in Appendix A. The particle content of the model (henceforth denoted as BLR) is then summarized in Table I.

III. Z' COUPLINGS TO FERMIONS

In this work, numerically, we use the SARAH program [19] to determine the vector and axial couplings of the fermions with the $Z'_{\rm BLR}$. This includes the full impact of gauge-kinetic mixing (GKM) as done in [14,18]. Considering this effect in full leads to $\sim\mathcal{O}(1)\%$ differences in vector and axial couplings. In this section, for simplicity, we neglect the impact of GKM but stress that all implications are considered in our final results.

We begin by examining the low-energy breaking of the gauge group in Eq. (5). The coupling of a fermion f to the $U(1)_R$ and $U(1)_{B-L}$ fields are obtained from

TABLE I. The particle content and generators of the $SU(3)_C \times SU(2)_L \times U(1)_R \times U(1)_{B-L}$ model.

Particle	T_{3L}	T_{3R}	T_{B-L}	T_χ	$Y = T_{3R} + T_{B-L}$	$Q = T_{3L} + Y$
$\begin{pmatrix} u \\ d \end{pmatrix}_L$	$+1/2$	0	$+1/6$	$+1/4$	$+1/6$	$+2/3$
	$-1/2$	0	$+1/6$	$+1/4$	$+1/6$	$-1/3$
u_R	0	$+1/2$	$+1/6$	$-1/4$	$+2/3$	$+2/3$
d_R	0	$-1/2$	$+1/6$	$+3/4$	$-1/3$	$-1/3$
$\begin{pmatrix} \nu_e \\ e^- \end{pmatrix}_L$	$+1/2$	0	$-1/2$	$-3/4$	$-1/2$	0
	$-1/2$	0	$-1/2$	$-3/4$	$-1/2$	-1
ν_R	0	$+1/2$	$-1/2$	$-5/4$	0	0
e_R	0	$-1/2$	$-1/2$	$-1/4$	-1	-1
χ_R^1	0	$-1/2$	$+1/2$	$+5/4$	0	0
χ_R^2	0	$+1/2$	$-1/2$	$-5/4$	0	0
S	0	0	0	0	0	0
$H \begin{cases} H_u = \begin{pmatrix} \phi_u^+ \\ \phi_u^0 \end{pmatrix}_L \\ H_d = \begin{pmatrix} \phi_d^0 \\ \phi_d^- \end{pmatrix}_L \end{cases}$	$+1/2$	$+1/2$	0	$-1/2$	$+1/2$	$+1$
	$-1/2$	$+1/2$	0	$-1/2$	$+1/2$	0
	$+1/2$	$-1/2$	0	$+1/2$	$-1/2$	0
	$-1/2$	$-1/2$	0	$+1/2$	$-1/2$	-1

$$-\mathcal{L}_{\rm BLR} = \bar{f}\gamma^\mu (g_R T_{3R} W^3_{\mu R} + g_{BL} T_{B-L} B^{BL}_\mu) f, \quad (10)$$

where $T_{B-L} = \frac{B-L}{2}$.

After symmetry breaking, these two fields will mix to become the SM massless hypercharge gauge boson, B_μ, and a massive Z'_μ (corresponding to the $Z'_{\rm BLR}$),

$$\begin{pmatrix} B^{BL}_\mu \\ W^3_{\mu R} \end{pmatrix} = \begin{pmatrix} \cos\theta_{BL} & -\sin\theta_{BL} \\ \sin\theta_{BL} & \cos\theta_{BL} \end{pmatrix} \begin{pmatrix} B_\mu \\ Z'_\mu \end{pmatrix}. \quad (11)$$

So, the $Z'_{\rm BLR}$ has the following coupling to fermions:

$$-\mathcal{L}^{Z'}_{\rm BLR} = Z'_\mu \bar{f}\gamma^\mu (g_R \cos\theta_{BL} T_{3R} - g_{BL} \sin\theta_{BL} T_{B-L}) f. \quad (12)$$

Since

$$g_R \sin\theta_{BL} = g_{BL} \cos\theta_{BL} = g_Y, \quad (13)$$

we may rewrite the Z' couplings of the BLR model in a more compact form,

$$\begin{aligned} -\mathcal{L}^{Z'}_{\rm BLR} &= Z'_\mu \bar{f}\gamma^\mu g_Y Q_{LR} f, \\ Q_{LR} &\equiv (\cot\theta_{BL} T_{3R} - \tan\theta_{BL} T_{B-L}), \\ \tan\theta_{BL} &= g_{BL}/g_R. \end{aligned} \quad (14)$$

We shall be interested in comparing the Z' couplings in the BLR model above to those in related models where the SM gauge group (including hypercharge) is augmented by an Abelian gauge group $U(1)'$, identified with the generator T_{BL}, resulting in the Z' couplings

$$-\mathcal{L}^{Z'}_{BL} = Z'_\mu \bar{f}\gamma^\mu g_{BL} T_{B-L} f, \quad (15)$$

TABLE II. Chiral couplings for the $U(1)_R$ and $U(1)_{B-L}$ models.

Model	ϵ^u_L	ϵ^u_R	ϵ^d_L	ϵ^d_R	ϵ^e_L	ϵ^e_R	ϵ^ν_L	ϵ^ν_R
T_{3R}	0	1/2	0	$-1/2$	0	$-1/2$	0	1/2
T_{B-L}	1/6	1/6	1/6	1/6	$-1/2$	$-1/2$	$-1/2$	$-1/2$

which may be compared to the BLR couplings in Eq. (14). We shall find to one-loop the non-GUT normalized couplings (i.e., in the conventions of this section).[1]

$$g_R = 0.448, \qquad g_{BL} = 0.459. \quad (16)$$

In general, the $Z'_{\rm BLR}$ couples to a fermion f which may be either left- or right-handed and the above couplings sum over both chiral components of all the fermions. For analyzing the couplings of different models, it is useful to decompose the couplings into either left-chiral or right-chiral components, leading to the vector and axial couplings in the BLR model as follows,

$$\begin{aligned} -\mathcal{L}^{Z'}_{\rm BLR} &= g_Y Z'_\mu \bar{f}\gamma^\mu (\epsilon^f_L P_L + \epsilon^f_R P_R) f \\ &= g_Y Z'_\mu \bar{f}\gamma^\mu \frac{1}{2} (g^f_V - g^f_A \gamma^5) f, \end{aligned} \quad (17)$$

where $P_{R,L} = (1 \pm \gamma_5)/2$ and the vector/axial couplings are defined as $g^f_{V/A} = \epsilon^f_L \pm e^f_R$. Similar decompositions can be made for the Z' couplings of the other models in Eq. (15). Table II shows the chiral couplings for the relevant generators T_R and $T_{B-L} = (B-L)/2$. Table III shows the

[1]Including GUT normalization, $\sqrt{3/2} g_{BL} = 0.563$. We also find the mixed couplings, related to GKM, $g_{R,BL} \sim g_{BL,R} \sim 0.01$.

TABLE III. Vector and axial couplings for the $U(1)_R$ and $U(1)_{B-L}$ models. Note that we have integrated out the right-handed neutrinos[2] in calculating g_V^ν and g_A^ν.

Model	g_V^u	g_A^u	g_V^d	g_A^d	g_V^e	g_A^e	g_V^ν	g_A^ν
T_{3R}	1/2	−1/2	−1/2	1/2	−1/2	1/2	0	0
T_{B-L}	1/3	0	1/3	0	−1	0	−1/2	−1/2

vector and axial couplings obtained for the two different models.

IV. Z' COUPLINGS TO HIGGS BOSONS

In this section, we shall ignore the $Z'_{\rm BLR}$ decays into bosons arising from χ_R^1 and χ_R^2. The χ_R^1 and χ_R^2 bosonic sector contains four degrees of freedom, two scalars plus two pseudoscalars, where one of the pseudoscalars is eaten by the $Z'_{\rm BLR}$, to leave two CP even scalars plus one CP odd pseudoscalar in the physical spectrum. If the soft masses of the χ_R^1 and χ_R^2 bosons are very large, then we would expect the physical CP odd pseudoscalar to become very heavy. This can be achieved by assuming a large soft mass term $B_{\mu_R}\chi_R^1\chi_R^2$ (the full superpotential and soft terms may be found in [14]). Since the $Z'_{\rm BLR}$ must decay into a scalar plus a pseudoscalar (assuming that CP and angular momentum are conserved) then this would imply that none of the bosons arising from χ_R^1 and χ_R^2 would be kinematically accessible in $Z'_{\rm BLR}$ decays.

Under the above assumption of large soft masses for χ_R^1 and χ_R^2, we shall discuss the $Z'_{\rm BLR}$ coupling to the Higgs bosons arising from H_u and H_d only, which are assumed to have smaller soft masses. To investigate the Z' coupling to what is essentially a 2-Higgs doublet model (2HDM) sector, we begin with the Lagrangian term with the covariant derivative

$$\mathcal{L}_{Z',\rm scalars} = (D_\mu\Phi_1)^\dagger(D_\mu\Phi_1) + (D_\mu\tilde{\Phi}_2)^\dagger(D_\mu\tilde{\Phi}_2) \quad (18)$$

with

$$D_\mu = \partial_\mu - i\frac{g_Y}{s_{BL}c_{BL}}\left(T_{3R} - s_{BL}^2\frac{Y}{2}\right), \quad (19)$$

where $\cos(\theta_{B-L}) \equiv c_{BL}$ and $\sin(\theta_{B-L}) \equiv s_{BL}$. Our two Higgs doublets are

[2]In the linear seesaw, the heavy neutrino mass is approximately $M_N \sim \tilde{F}v_R$, see Eq. (A1) in Appendix A for the definition of $\tilde{F}$ while v_R is the BLR breaking scale. We will see that the mass of the Z' is approximately $M_{Z'} \sim \frac{1}{2}\sqrt{(\frac{3}{2}g_{B-L}^2 + g_R^2)}v_R$. We, thus, prevent heavy neutrino decays ($2M_N > M_{Z'}$) through the requirement that the free Yukawa coupling be large enough, $\tilde{F} > \sqrt{(\frac{3}{2}g_{B-L}^2 + g_R^2)} \sim 0.2$.

TABLE IV. The coupling of the BLR Z' to the physical 2HDM mass states. The Feynman rule for the vertex is given by $(g_{Z'S_1S_2})(p-p')_\mu$, where p, p' are the momenta of the two scalars towards the vertex.

Vertex	$g_{Z'S_1S_2}$
$Z'h^0A^0$	$\frac{g_R\cos\theta_{B-L}\cos(\beta-\alpha)}{2}$
$Z'H^0A^0$	$\frac{-g_R\cos\theta_{B-L}\sin(\beta-\alpha)}{2}$
$Z'H^+H^-$	$-i\frac{g_R\cos\theta_{B-L}}{2}$

$$\Phi_1 = \begin{pmatrix} \phi_1^+ \\ (v_1 + h_1 + ia_1)/\sqrt{2} \end{pmatrix},$$
$$\tilde{\Phi}_2 = i\sigma_2\Phi_2^* = \begin{pmatrix} \phi_2^+ \\ (-v_2 - h_2 + ia_2)/\sqrt{2} \end{pmatrix}, \quad (20)$$

and we rotate the fields to the physical basis as in the standard 2HDM procedure,

$$\Phi_1^R = \begin{pmatrix} G^+ \\ (h^0 s_{\beta\alpha} + H^0 c_{\beta\alpha} + v_{\rm SM} + iG^0)/\sqrt{2} \end{pmatrix},$$
$$\tilde{\Phi}_2^R = \begin{pmatrix} H^+ \\ (-h^0 c_{\beta\alpha} + H^0 s_{\beta\alpha} + iA^0)/\sqrt{2} \end{pmatrix}, \quad (21)$$

where we defined the standard 2HDM rotation angles $\cos(\alpha-\beta) \equiv c_{\alpha\beta}$ and $\sin(\alpha-\beta) \equiv s_{\alpha\beta}$. We extract the physical couplings for our $Z'_{\rm BLR}$ to the h^0, H^0, $H^\pm$, A^0 in Table IV.

We find the partial widths by using the general expression for a Z' decaying into two spinless bosons of unequal masses M_1 and M_2, with coupling $g_{Z'S_1S_2}$ (read off from Table IV),

$$\Gamma(Z'_{\rm BLR} \to S_1S_2) = \frac{1}{48\pi}\frac{1}{M_{Z'}^3}g_{Z'S_1S_2}^2(M_{Z'}^4 + M_1^4 + M_2^4 - 2(M_2^2M_{Z'}^2 + M_1^2M_{Z'}^2 + M_1^2M_2^2)). \quad (22)$$

For a discussion of the Z'_{BL} coupling to the scalar sector in the $U(1)_{B-L}$ model, see e.g., [15].

V. RENORMALIZATION GROUP EQUATIONS

We now turn to the renormalization group equations (RGEs) at one loop. These RGEs will determine the $U(1)_R$ and $U(1)_{B-L}$ coupling constants and will also predict a value of the SM hypercharge coupling constant, given measured results of α_2 and α_3. We begin by using the SM β-function coefficients $b_2^{\rm SM} = -19/6$ and $b_3^{\rm SM} = -7$ for the $SU(2)_L$ and $SU(3)_c$ groups, respectively. We perform the running from M_Z up to our BLR breaking scale, which we denoted by v_R. From the scale $v_R < Q < v_{\rm SUSY}$, these two

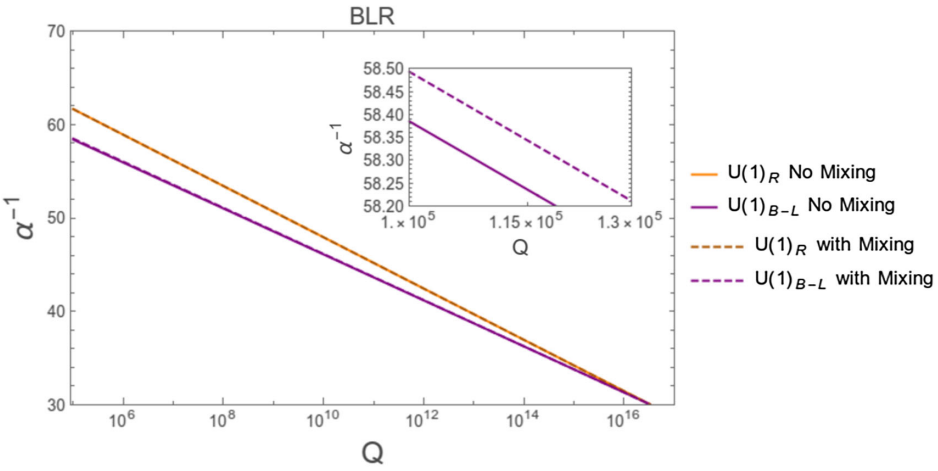

FIG. 1. Comparison of RGE evolution with (solid lines) and without (dashed lines) gauge-kinetic mixing from GUT to SUSY scale. The $U(1)_R$ evolution is unchanged, whereas the $U(1)_{B-L}$ is modified slightly. A zoomed in plot of this modification is shown.

β-function coefficients are unchanged, as none of the additional BLR particle content has quantum numbers under these two groups. Then, at $v_{\rm SUSY} < Q < M_{\rm GUT}$, we introduce the SUSY partners and the β-function coefficients are modified to $b_2^{\rm SUSY} = +1$ and $b_3^{\rm SUSY} = -3$. These are the familiar MSSM β-function coefficients. The strong and weak coupling constants are run until they intersect, which determines $Q = M_{\rm GUT}$ and $\alpha_{\rm GUT} \equiv \alpha_2(M_{\rm GUT}) = \alpha_3(M_{\rm GUT})$. We now run our $U(1)_{B-L}$ and $U(1)_R$ coupling constants down from this GUT scale.

As we have two $U(1)$ groups, they undergo GKM. We begin with the β-function coefficients $b_{BL}^{\rm BLR,SUSY} = 27/4$, $b_R^{\rm BLR,SUSY} = 15/2$ and a mixed term $b_{R,B-L}^{\rm BLR,SUSY} = -\sqrt{3/8}$, including a GUT normalization term of $3/8$ on the $U(1)_{B-L}$ and, hence, $\sqrt{3/8}$ on the $(U(1)_{B-L} \times U(1)_R)$ coefficient. Rotating the couplings into the upper triangular physical basis [20], and following the procedure of [21], we find the following β functions for the GUT normalized couplings,[3]

$$\frac{dg_R}{dt} = \frac{1}{(4\pi)^2}\frac{15 g_R^3}{2}, \tag{23}$$

$$\frac{d\tilde{g}}{dt} = \frac{1}{(4\pi)^2}\left[\left(\frac{27}{4}g_{BL}^2 - \sqrt{\frac{3}{2}}g_{BL}\tilde{g} + \frac{15}{2}\tilde{g}^2\right)\tilde{g} + \left(-\sqrt{\frac{3}{2}}g_{BL} + 15\tilde{g}\right)g_R^2\right], \tag{24}$$

$$\frac{dg_{BL}}{dt} = \frac{1}{(4\pi)^2}\left(\frac{27}{4}g_{BL}^2 - \sqrt{\frac{3}{2}}g_{BL}\tilde{g} + \frac{15}{2}\tilde{g}^2\right)g_{BL}. \tag{25}$$

[3]The couplings in this section are GUT normalized, while those in earlier sections are the non-GUT normalized couplings We have chosen the same nomenclature for both normalizations, being careful to specify which normalization we are using.

At the GUT scale, we set $\tilde{g} = 0$ and allow it to run to nonzero values at low scale. Figure 1 shows the running of the $U(1)_R$ and $U(1)_{B-L}$ groups both with (solid line) and without (dashed line) including the GKM procedure. One can see immediately that these two lines lie on top of one another, meaning the effect of the GKM is negligible. The α_R has an entirely negligible change and one can see a zoomed plot of the shift in the α_{BL} coefficient, which changes by $\mathcal{O}(0.1\%)$. At the low (TeV) scale, one finds a negligible mixing coupling term $\tilde{g} \approx 10^{-2}$; nevertheless, we include this correction in our numerical work.

We include GKM from the SUSY scale to the $U(1)_R \times U(1)_{B-L}$ breaking scale, v_R. From $v_R < Q < v_{\rm SUSY}$, decoupling the SUSY particles, the β-function coefficients change to $b_{BL}^{\rm BLR} = 17/4$, $b_R^{\rm BLR} = 13/3$ and a mixed term $b_{R,B-L}^{\rm BLR,SUSY} = b_{B-L,R}^{\rm BLR,SUSY} = -1/\sqrt{24}$. We summarize these beta function coefficients and their meaning in Appendix B. At v_R, these two coupling values determine the (GUT normalized) hypercharge coupling,

$$\alpha_1^{-1} = \frac{3}{5}\alpha_R^{-1} + \frac{2}{5}\alpha_{BL}^{-1}. \tag{26}$$

From this scale, α_1 is run further down from v_R to M_Z, with the SM β-function coefficient $b_1^{\rm SM} = 41/10$. The BLR breaking scale has been chosen such that the VEV and coupling values at this point correspond to a Z' with a statistical significance $\lesssim 2\sigma$, which is seen later to be 3750 GeV. Using this Z' mass, the v_R VEV is determined from the formula[4] [14] in the limit $\tilde{g} = 0$,

[4]The factor of $3/2$ in Eq. (27) multiplying g_{B-L}^2 comes from the $3/8$ GUT normalization factor times a factor of 4 in going from $B-L$ to $(B-L)/2$. This is responsible for the GUT scale prediction $\tan\theta_{BL} = g_{BL}/g_R = \sqrt{3/2}$ in terms of the non-GUT normalized couplings in Eq. (14).

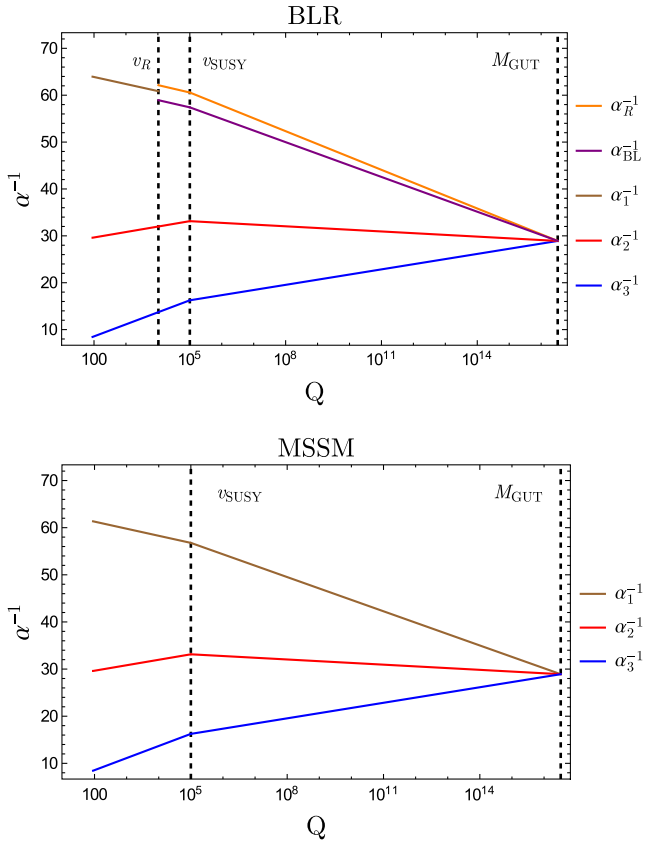

FIG. 2. The upper panel shows the running couplings in the BLR model, with $v_R = 11660$ GeV, which corresponds to $M_{Z'} = 3750$ GeV and $v_{\rm SUSY} = 10^5$ GeV. The GUT scale is determined to be $M_{\rm GUT} = 3.30 \times 10^{16}$ GeV. The lower panel shows the running couplings in the MSSM.

$$M_{Z'}^2 = \frac{1}{4}\left(\frac{3}{2}g_{B-L}^2 + g_R^2\right)v_R^2 + \frac{\frac{1}{4}g_R^4 v^2}{(3/2)g_{B-L}^2 + g_R^2} \approx \frac{1}{4}\left(\frac{3}{2}g_{B-L}^2 + g_R^2\right)v_R^2, \quad (27)$$

where $\sqrt{(3/2)}g_{B-L} = 0.563$, as seen in Eq. (16), and $M_{Z'} = 3750$ GeV leads to $v_R = 10328$ GeV.

The upper panel of Fig. 2 shows the running couplings of the BLR model, setting $v_R = 10328$ GeV and $v_{\rm SUSY} = 10^5$ GeV. Using our one-loop RGEs, we predict a value for the SM hypercharge coupling as $\alpha_Y(M_Z) = \frac{3}{5}\alpha_1(M_Z) = 1/102.44$, which we may compare to the experimentally determined value of $\alpha_Y^{\rm exp} = \frac{\alpha_{\rm EM}}{1-\sin^2\theta_W} = 1/98.39$ [22]. The difference between the two values may be partly accounted for by our procedure of running up the best fit experimental values of α_2 and α_3 at M_Z to determine $M_{\rm GUT}$ and $\alpha_{\rm GUT}$ at the point where they meet, then running all the gauge couplings from this point down to low energies. This procedure, though convenient for the BLR model where the hypercharge gauge coupling is not defined above v_R, does not take into account the experimental error in $\alpha_3^{\rm exp}$ in the prediction for $\alpha_Y^{\rm exp}$. Another source of error is the fact that we do not consider either two loop RGEs or threshold effects, both of which are beyond the scope of this paper. Using our one loop results, we determine the values of the couplings in Eq. (16), which refer to the non-GUT normalized couplings.

For comparison, the lower panel of Fig. 2 shows the MSSM at one-loop running couplings, again assuming $v_{\rm SUSY} = 10^5$ GeV. In this case, the analogous procedure to that used in the BLR model yields a prediction for the SM hypercharge coupling of $\alpha_Y^{\rm MSSM}(M_Z) = 1/102.25$.

VI. RESULTS

A. Preliminaries

In this section, we review the LHC results specific to the BLR model in Drell-Yan (DY) processes as well as in final states including Higgs bosons. We do so in two separate subsections to follow. In the case of DY studies, we also compare the BLR results to those of the $U(1)_{B-L}$ scenario. Throughout our analysis we assume the aforementioned heavy SUSY scale, thereby preventing decays of the Z' into sparticles. However, we consider the possibility that the 2HDM-like Higgs states of the BLR models are lighter than the Z', which may therefore decay into them via the couplings in Table IV. Further, notice that Z' decays into non-MSSM-like Higgs states can be heavily suppressed in comparison, in virtue of the fact that the additional CP-odd state not giving mass to the Z' can be made arbitrarily heavy (as previously explained), a setup which we assume here, so that we refrain from accounting for these decay patterns. Finally, recall that heavy neutrino decays are prevented here in the light of footnote 2 and that they have already been studied in, e.g., [23] (for the $B-L$ case), from where it is clear that they have little Z' diagnostic power. In contrast, we aim at making the point that the Higgs decays we study below can eventually be used for this purpose.

We use standard 2HDM notation, such that h^0 and H^0 are the CP-even Higgs mass states (with the lighter h^0 being the discovered SM-like one), A^0 the CP-odd one and $H^\pm$ the charged ones.

Table V summarizes the numerical values of the vector and axial couplings of the Z' to fermions for the $B-L$ and BLR models. For each scenario, we have defined new vector and axial couplings with the gauge coupling absorbed,

$$-\mathcal{L}^{Z'} = Z'_\mu \bar{f}\gamma^\mu \frac{1}{2}(\bar{g}_V^f - \bar{g}_A^f\gamma^5)f, \quad (28)$$

which may be compared to Eq. (17). For the $U(1)_{B-L}$ model, the calculation of $\bar{g}_{V,A}^f$ in Table V uses the gauge coupling constants shown there multiplied by the vector and axial couplings given previously in Table III. For the BLR model,

TABLE V. Numerical values of the vector and axial couplings for the $U(1)_{B-L}$ and $U(1)_{B-L} \times U(1)_R$ models. Note that we have decoupled the right-handed neutrinos in calculating g_V^ν and g_A^ν.

Model	Gauge coupling	$\bar{g}_V^u$	$\bar{g}_A^u$	$\bar{g}_V^d$	$\bar{g}_A^d$	$\bar{g}_V^e$	$\bar{g}_A^e$	$\bar{g}_V^\nu$	$\bar{g}_A^\nu$
$B-L$	$g_{BL} = 0.592$	0.197	0	0.197	0	−0.592	0	−0.296	−0.296
BLR	See Eq. (16)	−0.0103	−0.135	−0.279	0.135	0.300	0.135	0.217	0.217

the new numerical vector and axial couplings are derived including the full effects of gauge-kinetic mixing using SARAH (as a function of the mixed couplings $g_{BL,R}, g_{R,BL}$ and the rotation matrix which diagonalizes the neutral gauge boson mass matrices), but may be approximated analytically neglecting GKM using Eqs. (14) and (17) as

$$\bar{g}_{V,A}^f(\mathrm{BLR}) \approx g_Y[(\cot\theta_{BL})g_{V,A}^f(R) - (\tan\theta_{BL})g_{V,A}^f(BL)] \tag{29}$$

in terms of the vector and axial couplings $g_{V,A}^f(R)$ and $g_{V,A}^f(BL)$ for the T_{3R} and T_{B-L} models as written in Table III. The non-GUT normalized gauge couplings for the BLR model in Eq. (29) and Table V come from the RGE analysis leading to Eq. (16). The values of the non-GUT normalized gauge couplings g_{BL} and g_χ for the $B-L$ and χ models in Table V were taken from the low-energy parametrization in [8] rather than an RGE analysis, which would require us to specify the corresponding high-energy models, which we do not wish to do here, bearing in mind that the $B-L$ model does not emerge from $SO(10)$. If some other value of g_{BL} were used instead, then the vector and axial couplings for the $B-L$ model in Table V would be straightforwardly rescaled.

Many qualitative features of the results can be understood by examining the fermion couplings in Table V, for example, the vector nature of the $B-L$ couplings.

B. Drell-Yan

The most promising channel to search for and profile a Z' boson at the LHC in the BLR model is DY production and decay, namely, $pp \to \gamma, Z, Z' \to e^+e^-$ and $\mu^+\mu^-$. Figure 3(a) illustrates the current LHC reach (assuming 30 fb^{-1} of integrated luminosity at 13 TeV), highlighting that a Z' of BLR origin with a mass of 3750 GeV is allowed by data, as its statistical significance $\alpha \equiv \frac{|S|}{\sqrt{|S+B|}}$ is less than 2 in the entire mass range over which the signal $|S|$ could manifest itself over the background $|B|$. Notice that, here and in the following, our signal is given by the (modulus of the) cross section of $pp \to \gamma, Z, Z' \to e^+e^-$ and $\mu^+\mu^-$ minus that of $pp \to \gamma, Z \to e^+e^-$ and $\mu^+\mu^-$ (thereby including interference effects between Z' and γ, Z), the latter being the (irreducible) background.[5] This very same Z' boson will, however, become accessible by the end of Run 2 of the LHC, as illustrated in Fig. 3(b), where (assuming 300 fb^{-1} of integrated luminosity at 13 TeV) values of α in excess of 5 are found near the peak region.[6]

Once such a Z' signal is established, it will be necessary to diagnose it, i.e., to assess to which model it belongs. A useful variable in this respect is the (reconstructed) forward-backward asymmetry (A_{FB}^*) of the DY cross section. We use here the definition adopted in Ref. [28], see Sec. III therein, with no cut on the di-lepton rapidity (see also Refs. [29,30]). Figure 4 shows the shape of this observable at the LHC, for $\sqrt{s} = 13$ TeV and $M_{Z'} = 3750$ GeV, as it would appear in the Z' peak region of the di-lepton invariant mass distribution for the BLR model as well as the $U(1)_{B-L}$ scenario. The shape emerging from the BLR case is notably different from the one of the companion $SO(10)$ model[7]

In order to quantify whether the LHC will be able to differentiate these two models, from one another or the SM, one must include the statistical error in the formulation of A_{FB}^* [29]:

$$\delta A_{\mathrm{FB}} = \sqrt{\frac{1 - A_{\mathrm{FB}}^2}{N}}. \tag{30}$$

In Fig. 5, we include this error in a binned version of Fig. 4, which overlays the $U(1)_{B-L}$ and BLR models, for a luminosity of 3000 fb^{-1} corresponding to the final result for the High-Luminosity LHC (HL-LHC) run [31]. The purple region is the overlap of errors between the two models. One can see that there are areas where the errors do not overlap and, by looking at the entire invariant mass distribution, a detailed statistical analysis may in principle differentiate between these two models at this

[5]Notice that, for the Z' mass ranges currently allowed by experiment, other (reducible) backgrounds can be neglected.

[6]In performing this exercise, we have used the program described in Refs. [24,25] for the $U(1)_{B-L}$ case suitably adapted to the BLR one. In particular, our implementation accounts for Z' width and interference (with SM di-lepton production) effects, which tend to reduce somewhat the sensitivity of the LHC experiments. Needless to say, when these are neglected, we are able to reproduce results obtained by the LHC collaborations [26,27] with percent accuracy, for the corresponding choice of couplings (which differ somewhat from those used in the present paper). This is why our limits for Z' masses differ from those quoted by the LHC.

[7]As intimated, recall that the Z' couplings to leptons in the $U(1)_{B-L}$ case are purely vectorial, so that nonzero values of A_{FB}^* are due in this case to interference effects.

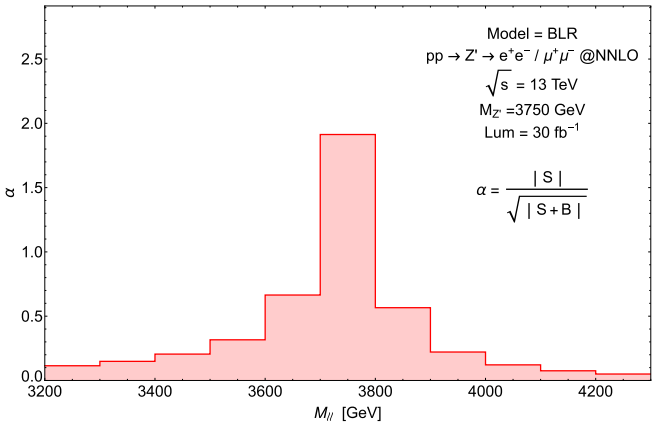

(a)

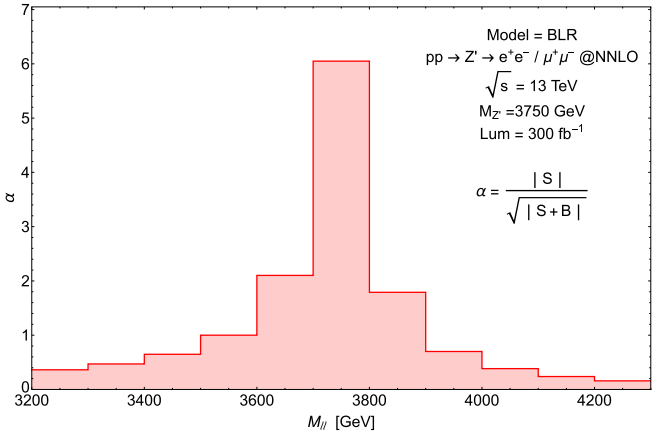

(b)

FIG. 3. Statistical significance for producing a Z' decaying into e^+e^- and $\mu^+\mu^-$ in the BLR model at integrated luminosities of (a) $L = 30$ fb^{-1} and (b) 300 fb^{-1}. The number of events obtained at these luminosities for $pp \to Z'$ is 74 in case (a) and 737 in case (b).

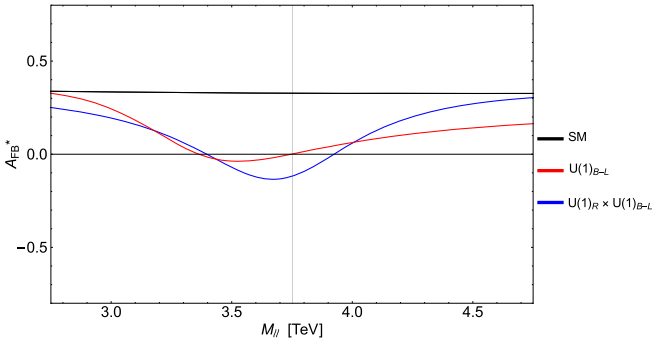

FIG. 4. The theoretical predictions of the leptonic forward-backward asymmetry at the LHC $A^*_{\rm FB}$ in the presence of a Z' decaying into e^+e^- and $\mu^+\mu^-$ for the $U(1)_Y \times U(1)_{B-L}$ (red) and $U(1)_R \times U(1)_{B-L}$ (blue) models. We have taken $M_{Z'} = 3750$ GeV. The SM (black) result is also given for comparison.

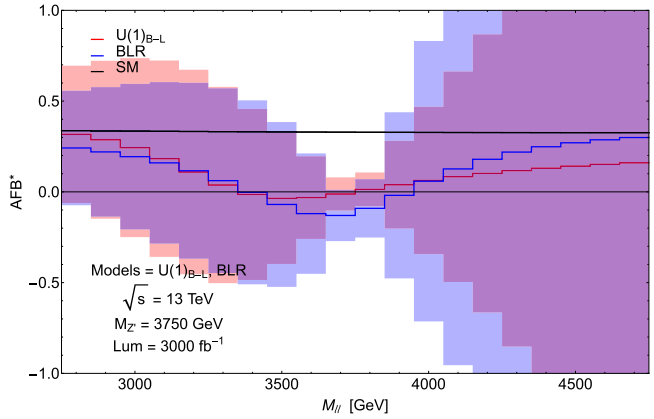

FIG. 5. The $A^*_{\rm FB}$ spectrum of the DY cross section in the presence of a Z' of mass $M_{Z'} = 3750$ GeV. The figure we shows the BLR model prediction for $A^*_{\rm FB}$ (in blue) and its error (shaded in light blue) as well as the $U(1)_{B-L}$ prediction for $A^*_{\rm FB}$ (in red) and its error (shaded in light red) as a function of the dilepton invariant mass. The purple region is the overlap of errors between the two models. Here, $L = 3000$ fb^{-1}.

luminosity, although we leave this task to the experimental collaborations.

C. Higgs final states

An alternative way of singling out the BLR nature of a Z' signal established via DY studies would the one pursuing the isolation of its exotic decays, i.e., into non-SM objects. Under the enforced assumption of heavy neutrinos, additional CP-odd Higgs boson and all sparticles being (much) heavier than the Z', the latter would include those into all possible MSSM-like (pseudo)scalar states pertaining to the Higgs sector of the BLR model, which, as discussed in Table I, is notably different from those of the $U(1)_{B-L}$ scenario. In particular, in the presence of CP conservation, the following decay channels would be allowed in the BLR framework: $Z' \to A^0 h^0$, $A^0 H^0$ and

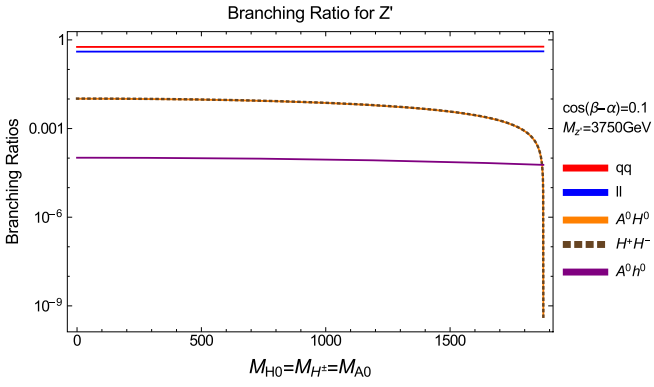

FIG. 6. BRs of a Z' in the BLR model as a function of degenerate A_0, H^0 and $H^\pm$ masses. Here, $M_{Z'} = 3750$ GeV and $\cos(\beta - \alpha) = 0.1$.

H^+H^-. These are presented for the usual Z' benchmark, assuming $\cos(\beta-\alpha)=0.1$ (so as to comply with LHC data from Higgs studies), in Fig. 6, for representative values of the Higgs boson masses. While the corresponding BRs are always subleading (of $\mathcal{O}(10^{-4})$ to $\mathcal{O}(10^{-2})$) with respect to those of the decays into SM fermions, the (on-shell) Z' cross section is 2.46 fb, so that HL-HLC luminosities should render the extraction of these decay modes possible, whichever the final decay patterns of the Higgs bosons involved.

VII. CONCLUSION

$SO(10)$ GUTs have the remarkable property that they predict right-handed neutrinos, making neutrino mass inevitable. $SO(10)$ is also a rank 5 gauge group, which implies that any rank preserving GUT breaking sector will lead to an extra Abelian factor in the low-energy effective theory, which protects right-handed neutrinos from gaining mass. If the rank is broken at the TeV scale, then there will be a Z' and massive right-handed neutrinos possibly observable at the LHC.

We have considered $SO(10)$ motivated Z' models. In particular, we have focused on the breaking pattern in Eq. (3), where the final breaking scale in Eq. (5), of the $U(1)_R\times U(1)_{B-L}$ Abelian subgroup into the hypercharge $U(1)_Y$ of the SM, may be around the TeV scale without spoiling gauge unification, within the accuracy of our one-loop analysis. The SUSY version of the $U(1)_R\times U(1)_{B-L}$ (BLR) model permits a linear seesaw mechanism for neutrino mass generation.

After defining the BLR model particle content and giving the relevant $Z'_{\rm BLR}$ and Higgs couplings, we have focused on the discovery prospects of the $Z'_{\rm BLR}$ at the LHC, its decay into Higgs states, and the forward-backward asymmetry as a diagnostic for discriminating it from the Z'_{BL} of the $U(1)_Y\times U(1)_{B-L}$ model. It is noteworthy that the Z'_{BL} of the $B-L$ model has purely vector couplings to quarks and leptons, making the forward-backward asymmetry a powerful discriminator, as we have discussed. In general, we have set out to test whether such models can be disentangled at past (like LEP/SLC) and present (like LHC) machines, assuming that the SUSY scale is higher than the $Z'_{\rm BLR}$ mass.

Having determined the parameters of the BLR model to one-loop accuracy at the TeV scale, we have examined the feasibility of the LHC to extract a $Z'_{\rm BLR}$ signal. We have shown that $Z'_{\rm BLR}$ mass values just below the current sensitivity of the LHC can easily be accessed by the end of Run 2 in standard DY searches exploiting electron and muon final states. Furthermore, we have made a detailed investigation of $A^*_{\rm FB}$ (i.e., the reconstructed forward-backward asymmetry) of these di-lepton final states and shown that it may be possible to distinguish the $Z'_{\rm BLR}$ of the $U(1)_R\times U(1)_{B-L}$ from the Z'_{BL} of the $U(1)_Y\times U(1)_{B-L}$ case, assuming HL-LHC luminosities. This is probably the main new result of this paper.

We have also considered the $Z'_{\rm BLR}$ decays into MSSM-like Higgs bosons, which would include $Z'_{\rm BLR}\to A^0h^0$, A^0H^0 and H^+H^-, but excluding possible decays into χ^1_R and χ^2_R bosons which we assume to be too heavy to be produced. While the Higgs decay rates are always small, from percent to fraction of permille level, compared to those into SM leptons and quarks, HL-HLC luminosities should render the extraction of all of these signals feasible. Though such decays are often neglected in the literature, they provide an additional Higgs production mechanism, possibly the dominant mechanism on the $Z'_{\rm BLR}$ resonance at an e^+e^- collider, and a crucial test of the gauge structure of the model in the 2HDM versions of the models that SUSY demands.

ACKNOWLEDGMENTS

S. M. is supported in part through the NExT Institute. All authors acknowledge support from Grant No. H2020-MSCA-RISE-2014 No. 645722 (NonMinimalHiggs), the European Union's Horizon 2020 Research and Innovation program under Marie Skłodowska-Curie Grant agreements Elusives ITN No. 674896 and InvisiblesPlus RISE No. 690575. S. J. D. K. would like to thank Luigi Delle Rose and Ronald Rodgers for useful discussions. Finally, we thank Juri Fiaschi for discussion and numerical help.

APPENDIX A: LINEAR SAW

The linear seesaw is similar to an inverse seesaw, but with $\mu\to 0$ and a new term coupling a left-handed (LH) neutrino to the scalar singlet S:

$$\begin{pmatrix} 0 & Yv & Fv_L \\ Y^Tv & 0 & \tilde{F}v_R \\ F^Tv_L & \tilde{F}^Tv_R & 0 \end{pmatrix} \equiv \begin{pmatrix} 0 & m_D & \epsilon \\ m_D^T & 0 & M_\chi \\ \epsilon^T & M_\chi^T & 0 \end{pmatrix}. \quad \text{(A1)}$$

Each element here corresponds to a 3×3 block. Solving this in block diagonal form, assuming $\epsilon \ll m_D \ll M_\chi$, one finds

$$\begin{pmatrix} M_\chi + m_D^T m_D M_\chi^{-1} & 0 & 0 \\ 0 & -(M_\chi + m_D^T m_D M_\chi^{-1}) & 0 \\ 0 & 0 & -\epsilon\frac{m_D^T}{M_\chi} \end{pmatrix}. \quad \text{(A2)}$$

So the light and heavy physical masses are

$$M_{\nu_L} = -\epsilon\frac{m_D^T}{M_\chi} + \text{H.c.} \quad \text{(A3)}$$

$$M_{N_1} \sim M_{N_2} \sim M_\chi + m_D^T m_D M_\chi^{-1} + \text{H.c.} \quad \text{(A4)}$$

Here we have the light neutrinos, ν_L, as observed in oscillation experiments, and $N_{1,2}$ are the heavier neutral fermions. The smallness of ϵ may allow for a low (TeV) scale M_χ, which is a fundamental feature of all low-scale seesaw mechanisms. Unlike the inverse seesaw, we see that M_{ν_l} is linear in m_D, which is proportional to the Yukawa couplings, hence the name "linear" seesaw.

APPENDIX B: RGES

Beta functions for the non-Abelian and Abelian groups, respectively, are [21]

$$\frac{\mathrm{d}g_a}{\mathrm{d}t} = \frac{B_a g_a^3}{16\pi^2}, \qquad \frac{dg_{lm}}{dt} = \frac{g_{lk}}{16\pi^2} b_{ij} g_{ik} g_{jm}, \tag{B1}$$

where the index a runs over the non-Abelian groups $SU(2)_L$ and $SU(3)_c$, $a = 2, 3$ and (i, j, k, l, m) run over the $U(1)_R, U(1)_{B-L}$, and mixed $U(1)_R \times U(1)_{B-L}$ and $U(1)_{B-L} \times U(1)_R$ groups, $(i, j, k, l, m) = (R, B-L)$ and Einstein summation convention is assumed. For our RGE section, we make a rotation on the coupling matrix G, such that it is set in upper triangular form [20]

$$G = \begin{pmatrix} g_{11} & g_{12} \\ g_{21} & g_{22} \end{pmatrix} \tag{B2}$$

$$\tilde{G} = GO_R^T = \begin{pmatrix} g & \tilde{g} \\ 0 & g' \end{pmatrix} = \begin{pmatrix} \frac{g_{11}g_{22}-g_{12}g_{21}}{\sqrt{g_{21}^2+g_{22}^2}} & \frac{g_{11}g_{21}+g_{12}g_{22}}{\sqrt{g_{21}^2+g_{22}^2}} \\ 0 & \sqrt{g_{21}^2+g_{22}^2} \end{pmatrix}. \tag{B3}$$

One may consequently find the RGE in terms of $g, g', \tilde{g}$ by differentiating these expressions and then replacing the differentials dg_{ij}/dt with the beta functions as calculated with Eq. (B1), then replacing g_{11}, g_{12}, g_{22} in terms of $g, g', \tilde{g}$. The beta function coefficients are given in Table VI.

TABLE VI. Beta function coefficients for Abelian and non-Abelian gauge groups in the BLR model.

Coefficient	GUT normalisation	Value	Scale	
$b_{R,R}^{BLR}$	1	15/2	$M_{\mathrm{SUSY}} < Q < M_{\mathrm{GUT}}$	Abelian
		13/3	$M_{\mathrm{BLR}} < Q < M_{\mathrm{SUSY}}$	
$b_{(B-L),(B-L)}^{BLR}$	3/8	27/4	$M_{\mathrm{SUSY}} < Q < M_{\mathrm{GUT}}$	
		17/4	$M_{\mathrm{BLR}} < Q < M_{\mathrm{SUSY}}$	
$b_{R,B-L}^{BLR} = b_{B-L,R}^{BLR}$	$\sqrt{3/8}$	$-\sqrt{3/8}$	$M_{\mathrm{SUSY}} < Q < M_{\mathrm{GUT}}$	
		$-1/\sqrt{24}$	$M_{\mathrm{BLR}} < Q < M_{\mathrm{SUSY}}$	
B_3^{BLR}	1	-3	$M_{\mathrm{SUSY}} < Q < M_{\mathrm{GUT}}$	Non-Abelian
	1	-7	$M_{\mathrm{BLR}} < Q < M_{\mathrm{SUSY}}$	
	1	-7	$M_{\mathrm{EW}} < Q < M_{\mathrm{BLR}}$	
B_2^{BLR}	1	1	$M_{\mathrm{SUSY}} < Q < M_{\mathrm{GUT}}$	
	1	-19/6	$M_{\mathrm{BLR}} < Q < M_{\mathrm{SUSY}}$	
	1	-19/6	$M_{\mathrm{EW}} < Q < M_{\mathrm{BLR}}$	

[1] S. F. King, J. High Energy Phys. 08 (2017) 019; B. S. Acharya, K. Bozek, M. Crispim Romao, S. F. King, and C. Pongkitivanichkul, J. High Energy Phys. 11 (2016) 173.
[2] S. F. King and T. Yanagida, Prog. Theor. Phys. **114**, 10035 (2006).
[3] S. Khalil and A. Masiero, Phys. Lett. B **665**, 374 (2008).
[4] P. F. Perez and S. Spinner, Phys. Rev. D **83**, 035004 (2011).
[5] B. O'Leary, W. Porod, and F. Staub, J. High Energy Phys. 05 (2012) 042.
[6] A. Elsayed, S. Khalil, and S. Moretti, Phys. Lett. B **715**, 208 (2012).
[7] G. Arcadi, M. Lindner, Y. Mambrini, M. Pierre, and F. S. Queiroz, Phys. Lett. B **771**, 508 (2017).
[8] E. Accomando, A. Belyaev, L. Fedeli, S. F. King, and C. Shepherd-Themistocleous, Phys. Rev. D **83**, 075012 (2011).
[9] P. Langacker, Rev. Mod. Phys. **81**, 1199 (2009).
[10] M. Malinsky, J. C. Romao, and J. W. F. Valle, Phys. Rev. Lett. **95**, 161801 (2005).
[11] M. Hirsch, S. Morisi, and J. W. F. Valle, Phys. Lett. B **679**, 454 (2009).
[12] V. De Romeri, M. Hirsch, and M. Malinsky, Phys. Rev. D **84**, 053012 (2011).
[13] M. Hirsch, M. Malinsky, W. Porod, L. Reichert, and F. Staub, J. High Energy Phys. 02 (2012) 084.
[14] M. Hirsch, W. Porod, L. Reichert, and F. Staub, Phys. Rev. D **86**, 093018 (2012).
[15] L. Basso, A. Belyaev, D. Chowdhury, M. Hirsch, S. Khalil, S. Moretti, B. O'Leary, W. Porod, and F. Staub, Comput. Phys. Commun. **184**, 698 (2013).
[16] M. Frank and O. Ozdal, arXiv:1709.04012.
[17] J. Chakrabortty and A. Raychaudhuri, Phys. Rev. D **81**, 055004 (2010); **97**, 095010 (2018).
[18] M. E. Krauss, W. Porod, and F. Staub, Phys. Rev. D **88**, 015014 (2013).
[19] F. Staub, Comput. Phys. Commun. **185**, 1773 (2014).
[20] C. Coriano, L. Delle Rose, and C. Marzo, J. High Energy Phys. 02 (2016) 135.
[21] S. Bertolini, L. Di Luzio, and M. Malinsky, Phys. Rev. D **80**, 015013 (2009).
[22] C. Patrignani *et al.* (Particle Data Group), Chin. Phys. C **40**, 100001 (2016).
[23] S. Khalil and S. Moretti, Rep. Prog. Phys. **80**, 036201 (2017).
[24] W. Abdallah, J. Fiaschi, S. Khalil, and S. Moretti, Phys. Rev. D **92**, 055029 (2015).
[25] W. Abdallah, J. Fiaschi, S. Khalil, and S. Moretti, J. High Energy Phys. 02 (2016) 157.
[26] M. Aaboud *et al.* (ATLAS Collaboration), Phys. Lett. B **761**, 372 (2016).
[27] V. Khachatryan *et al.* (CMS Collaboration), Phys. Lett. B **768**, 57 (2017).
[28] E. Accomando, A. Belyaev, J. Fiaschi, K. Mimasu, S. Moretti, and C. Shepherd-Themistocleous, J. High Energy Phys. 01 (2016) 127; E. Accomando, D. Becciolini, A. Belyaev, S. Moretti, and C. Shepherd-Themistocleous, J. High Energy Phys. 10 (**2013**) 153.
[29] E. Accomando, A. Belyaev, J. Fiaschi, K. Mimasu, S. Moretti, and C. Shepherd-Themistocleous, Nuovo Cimento Soc. Ital. Fis. C **38**, 153 (2016).
[30] J. Fiaschi, E. Accomando, A. Belyaev, K. Mimasu, S. Moretti, and C. H. Shepherd-Themistocleous, Proc. Sci. EPS-HEP2015 (**2015**) 176 [arXiv:1510.05892].
[31] F. Gianotti *et al.*, Eur. Phys. J. C **39**, 293 (2005).